Wideband Decoupled 8-Element MIMO Mobile Phone Antenna for Sub-6GHz 5G NR Bands

Jiagang He, Shichao Zhu, Jie Yu, Hao Li, and Gaosheng Li

College of Electrical and Information Engineering
Hunan University, Changsha, 410082, China
Gaosheng7070@vip.163.com

Abstract **–** A broadband decoupled dual antenna pair suitable for sub-6G mobile terminal application is proposed and designed. The multiple input multiple output (MIMO) antenna pair is arranged on the metal frame of the mobile phone, with two antenna pairs on each metal frame. The slotted antenna element structure and defect ground decoupling structure are used to achieve wide band and high isolation. Based on the decoupled antenna pair, an eight-element MIMO antenna is designed. Similarly, the coupling between antenna pairs is effectively reduced by etching the decoupled defect structure of a zigzag shape on the system surface. The prototype of the antenna array is successfully fabricated and tested. Simulation and experimental results show that the proposed eight-element MIMO antenna can fully cover the n77/n78/n79 band of 5G New Radio and 5 GHz band of WLAN. The overall efficiency of the antenna is 50%-75%, the envelope correlation coefficient (ECC) is below 0.08, and the isolation between any two ports is better than 11 dB.

Index Terms **–** 5G New Radio (5G NR), metal-frame smartphone, multiple-input–multiple-output (MIMO) antenna, slot antenna, WLAN 5 GHz band.

I. INTRODUCTION

Multiple input multiple output (MIMO) technology, as one of the core technologies of future fifth generation (5G) communication systems, can significantly improve spectral efficiency without increasing power and spectrum. Therefore, it is widely used in the design of terminal antennas to improve performance and adapt to 5G communication. The fourth generation (4G) mobile communication system, also known as LTE (Long Term Evolution), introduces MIMO technology to improve the transceiver efficiency of wireless mobile communication networks, and can effectively improve channel capacity and spectrum efficiency. As (5G) mobile communications enter the commercial phase, there will be greater data capacity, higher data transmission rates and lower delays. In order to achieve these difficult goals, more challenging requirements are put on the corresponding antenna design.

According to technical specification 38.101 of the 3G Partner Program, FR1 is the 5G NR band operating below 6 GHz (or less), while FR2 is the 5G NR band operating in millimeter-wave [1]. The design of millimeter-wave antenna is mainly faced with the serious problem of spatial attenuation, which is not discussed here [2]. In bands below 6 GHz, 3G/4G mobile communication systems now use bands below 3 GHz, while bands between 5 and 6 GHz are now used in WLAN 5 GHz bands (5150-5825 MHz). For 5G networks, 5G NR bands for n77 (3300-4200 MHz), n78 (3300-3800 MHz) and n79 (4400-5000 MHz) are planned. At present, 5G antenna design in the band below 6 GHz faces the bottleneck of limited bandwidth and needs to be expanded. For mobile terminal applications, early antenna designs below 6 GHz were concentrated in 3.4-3.6 GHz or 3.3-3.8 GHz, with relatively limited bandwidth [3–7]. Dual-band antennas covering 3.3-3.8 GHz and other bands below 6 GHz are studied in [8–11]. Recently, [12–14] antennas have been proposed to fully cover 5G NR bands n77 (3300-4200 MHz), n78 (3300-3800 MHz), and n79 (4400-5000 MHz). Still, their bandwidth is expected to expand further.

A simple design scheme for 5G MIMO smartphone antennas is to place 4 or 8 antenna units in different areas of the smartphone [2–26]. Due to the limited space, the coupling effect between elements is usually the focus of attention, and it is difficult to achieve decoupling between them. In recent years, there has been much research on terminal antenna decoupling. For example, neutralization line [15] is a common decoupling technique, but it tends to work only in narrow bands. In [8], spatial orthogonal decoupling is achieved by placing units at four corners of the substrate. In addition, some other decoupling technologies, such as defective ground structure [16–17], decoupling unit [18] and self-isolation unit [19–22], lumped element loading [23], and differential feed [24], are also studied to further improve the

Submitted On: June 22, 2022
Accepted On: August 30, 2022

https://doi.org/10.13052/2022.ACES.J.371204

isolation performance. Although these various decoupling technologies improve the isolation performance of antenna elements, they also occupy a lot of space resources. Therefore, how to simplify the design of the decoupling structure so as to improve the isolation degree between units and reduce the occupation of space resources has become a topic worthy of study.

This paper proposes a decoupled dual antenna pair for sub-6G smartphone applications. According to the design requirements of the combination of modern smart phone antenna and metal frame, four antenna pairs are gathered on the mobile terminal to form a broadband eight-element MIMO antenna array. The prototype of MIMO antenna array is fabricated and tested. In addition to covering 5G NR n77/n78/n79 bands, the array can also work in the 5 GHz (5170-5835 MHz) band of WLAN. The isolation performance in the whole working band is better than 11 dB, which can well meet the requirements of 5G terminal antenna. The measured results agree well with the simulation results.

II. ANTENNA DESIGN AND GEOMETRY

A. Geometry of proposed antenna

Figure 1 is a schematic diagram of an eight-element MIMO mobile phone antenna proposed in this paper. All antenna elements are located on the two long frames of the mobile phone. The size of the main substrate of the system adopts the general specifications of mobile phones in the contemporary market, and the size is 150 mm x 75 mm. The size of the two small substrates is 150 mm x 7 mm, they are placed vertically on both sides of the main substrate, and four antenna units are placed on each small substrate. The material used for the main substrate and the small substrate are FR-4, the substrate thickness is 0.8 mm, the relative dielectric constant ε_r is 4.3, and the loss angle tangent tan δ is 0.025. Figure 2 shows the structure diagram of the antenna pair in the mobile phone antenna. It can be seen from the figure that the antenna unit consists of an open slot in a small substrate and a slot in the floor. The antenna structure is fed by coupling L-shaped feeder branches on the substrate. The two antenna elements in the antenna pair are also arranged with respect to the decoupled structure. The decoupling between the compact antenna pairs is realized by a slotted structure designed with a zigzag shape. The values of each structural parameter in the antenna structure are given in Table 1. Each antenna is fed from the back of the substrate by an SMA connector through a hole connected to the microstrip line.

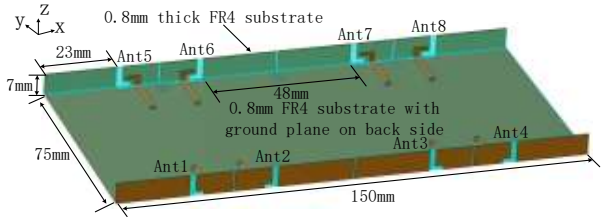

Fig. 1. Schematic diagram of eight-element MIMO mobile phone antenna.

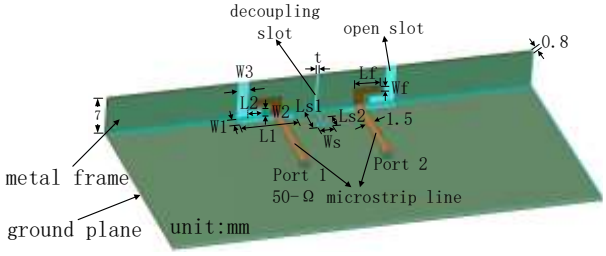

Fig. 2. Structure diagram of compact antenna pair.

Table 1: Antenna element size / mm

W1	W2	W3	Ws	Wf	L1	L2
2	1.5	2	2.5	1	10	2.5
Ls1	Ls2	Lf	t			
5.5	3	4.5	0.5			

B. Design process and analysis

The structural design comparison of MIMO mobile phone antenna designed in this paper is shown in Fig. 3. In order to clearly show the performance advantages brought by the antenna structure that we finally designed, Fig. 4 shows the comparison of S parameters under three different antenna design forms. Compared with the structure of antenna 1, the proposed antenna structure has one more rectangular slot on the side small substrate, and the antenna unit is an L-shaped slot when viewed from the side. Antenna 2 does not have a zigzag slot between two compact antenna pairs. As can be seen from the comparison of S parameters of the three antenna designs in Fig. 4, the -6 dB impedance bandwidth of antenna 1 is relatively narrow, mainly reflected by the fact that the coverage range of the frequency band just covers the critical value of the low frequency band. Moreover, due to the existence of the decoupling structure in its design, the element isolation degree of antenna 1 is relatively ideal. The -6 dB impedance bandwidth of antenna 2 is relatively wide, especially in the lower frequency band. However, due to the absence of a decoupling structure, the isolation degree between elements is relatively low, which is also a reason for its wide impedance bandwidth in the lower frequency band. It can be seen from the simulation results of S parameters that the -6 dB impedance bandwidth of the proposed antenna is wider than that of antenna 1 without a rectangular slot on the small substrate. Compared with antenna 2 without the decoupling

structure, the isolation degree between elements of the proposed antenna is higher than 10 dB, which is about 5 dB higher.

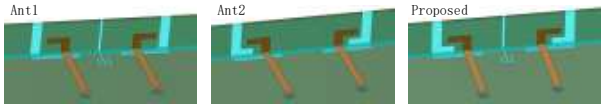

Fig. 3. Design evolution process of antenna structure.

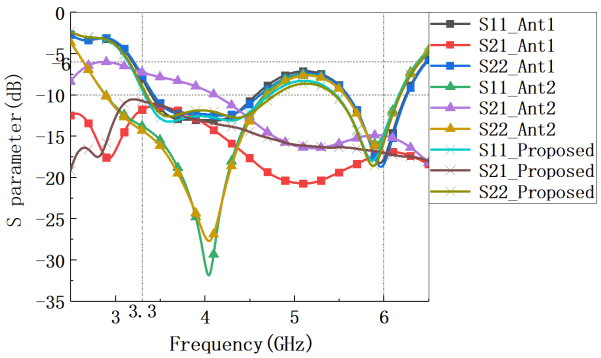

Fig. 4. Comparison of S parameters in structural design of antenna pairs.

III. RESULTS AND DISCUSSION

A. Current distribution

In order to understand the decoupling principle of the proposed antenna more intuitively, Figs. 5 (a) and (b) show the electric field and current distribution of the open slot antenna at the resonant frequency 3.78 GHz and 5.85 GHz, respectively. It can be seen from Fig. 5 that there is a maximum electric field at the open end of the open slot antenna and a null electric field at the shorted end of the open slot antenna. It is obvious that a quarter-wavelength slot mode is excited within the open slot. At the two different resonant frequencies, the electric field direction in the open slot is opposite, and the current distribution is different. The current distribution at resonant frequency f2=5.85 GHz has a current null point, so different resonances are generated.

Figure 6 shows the comparison of surface current distribution between antenna pairs at 3.78 GHz with or without a decoupling structure. Similarly, the decoupling effect also exists in the whole operating frequency band of the antenna. As can be seen from Fig. 6, when there is no designed decoupling structure between compact antenna pairs, the current fed from one port will be coupled from antenna 1 to antenna 2, resulting in a large current flowing on antenna 2. However, when the designed decoupling structure exists, the coupling current basically flows through the designed decoupling structure with a zigzag shape, making the coupling current on antenna 2 virtually absent, so as to achieve a better isolation effect between antenna pairs.

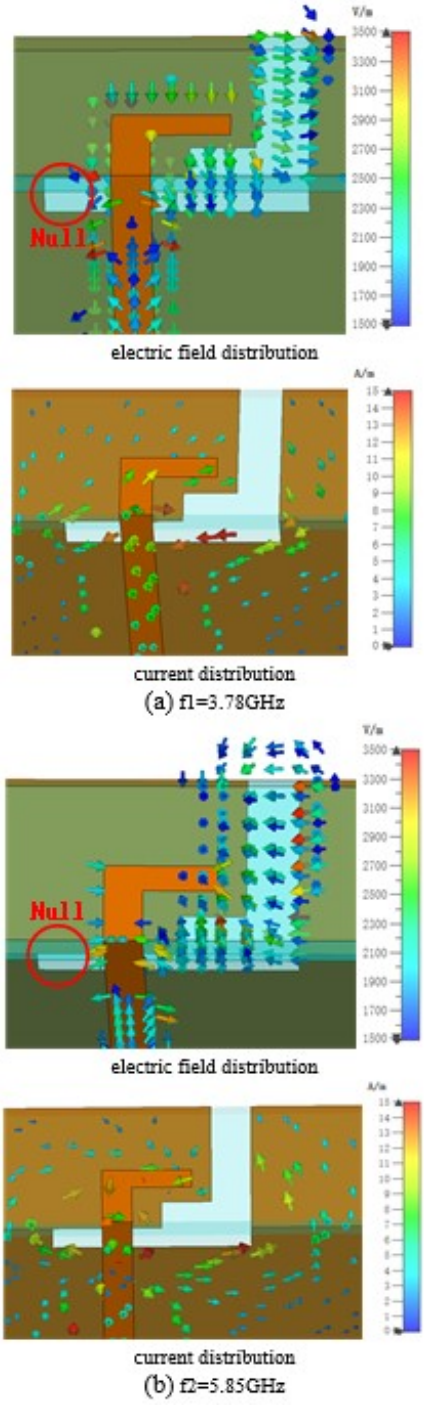

Fig. 5. Electric field distribution and current distribution of antenna element at (a) f1=3.78 GHz and (b) f2=5.85 GHz.

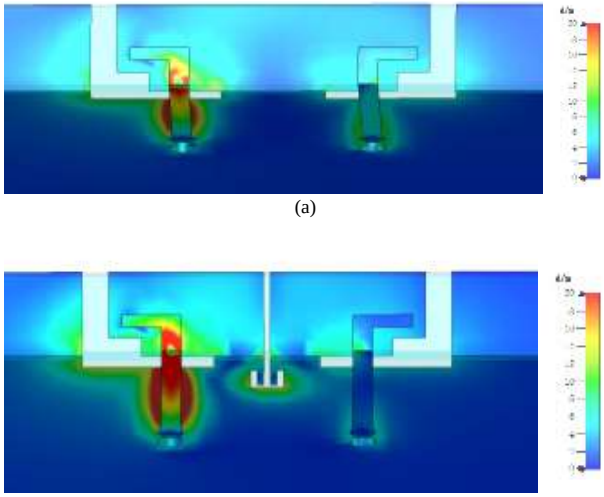

(a) (b)

Fig. 6. Comparison of surface current distribution of antenna pairs at 3.78GHz. (a) There is no decoupling structure. (b) There are decoupling structures.

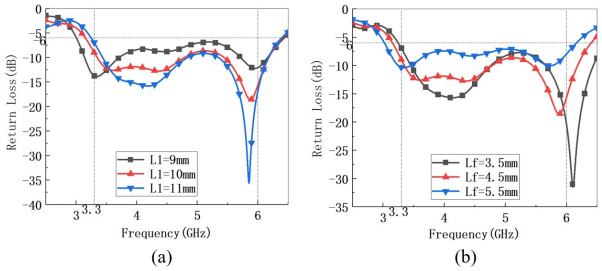

(a) (b)

Fig. 7. The return loss of antenna unit varies with (a) L1 and (b) Lf.

B. Parameter analysis

In this section, the effects of some important parameters on the performance of the antenna are analyzed. The influence results of the length L1 of antenna unit slot and L-type coupling feed branch length Lf on the return loss of the antenna unit are shown in Figs. 7 (a) and (b) respectively. As can be seen from the figure, with the increase of the length L1 of the antenna unit slot, the corresponding lower resonant frequency point moves to the high frequency, and the −6 dB impedance bandwidth is also reduced at this time. However, with the increase of L-type coupling feed branch length Lf, the overall resonant depth of the antenna decreases, that is, the Q value decreases, and the resonance point at the low frequency also moves to the lower frequency band. Therefore, L1=10 mm and Lf=4.5 mm are taken in combination with the effects of the two parameters on the overall performance of the antenna. Figures 8 (a) and (b) respectively show the influence of two key parameters Ls1 and Ls2 in the decoupling structure of antenna pair on the return loss of antenna unit itself and the isolation degree between units. As can be seen from the figure, the impedance bandwidth of the corresponding low frequency band becomes wider with the increase of the length Ls1 of the zigzag shape decoupling slot, but the isolation degree between the corresponding antenna pairs also decreases. Similarly, with the increase of the length Ls2 of the zigzag shape decoupling slot, the impedance bandwidth of the corresponding low frequency band also becomes wider, while the isolation degree between the corresponding antenna pairs also decreases. Therefore, Ls1=5.5 mm and Ls2=3 mm in combination with the effects of the two parameters on the overall performance of the antenna.

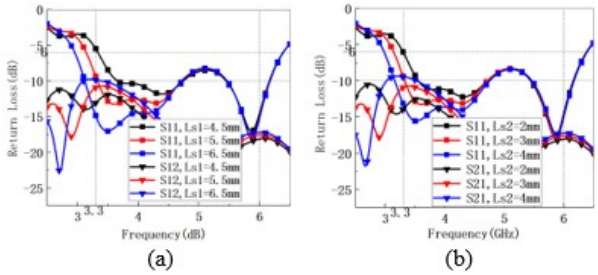

(a) (b)

Fig. 8. The return loss of antenna unit varies with (a) Ls1 and (b) Ls2.

C. Test results

In order to better analyze the performance of the sub-6G MIMO mobile phone antenna proposed in this paper, according to the specific size of the antenna model given in Table 1, physical production and testing of the antenna model were carried out. Figure 9 is a physical picture of the antenna. The test results were compared with the simulation results, the comparison of simulation and test results of reflection coefficient S11 and transmission coefficient S21 of this eight-element MIMO antenna is shown in Figs. 10 and 11 respectively. Due to the symmetry of the antenna structure, only necessary results are given in the figure. As can be seen from Fig. 10, the antenna system can well cover the sub-6G (3.3-6 GHz) full frequency band, and the simulation results are in good agreement with the measured results. As can be seen from Fig. 11, the isolation degree between the eight antennas is all better than 10 dB, which basically meets the requirements of the antenna unit isolation degree of MIMO mobile phone antennas. The isolation degree of antenna units mainly depends on the isolation degree between antenna pairs and antenna pairs on the same frame small substrate and the isolation degree between antenna pairs.

Figure 12 shows the simulation and measured comparison results of the total efficiency of MIMO mobile

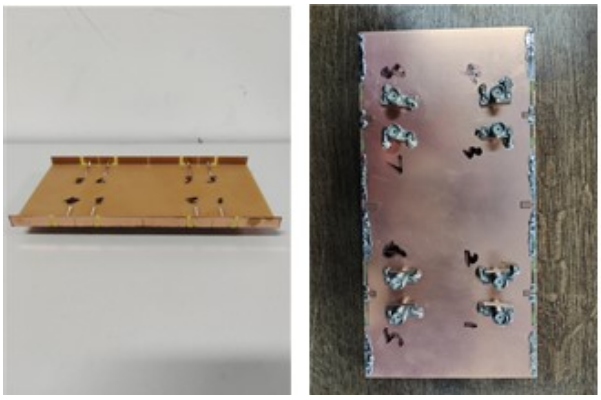

Fig. 9. Photograph of the fabricated prototype.

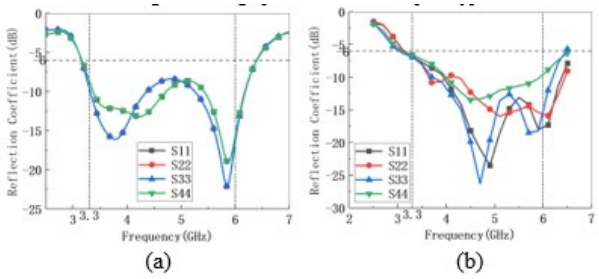

Fig. 10. Reflection coefficients of Ants1-4. (a) Simulated. (b) Measured.

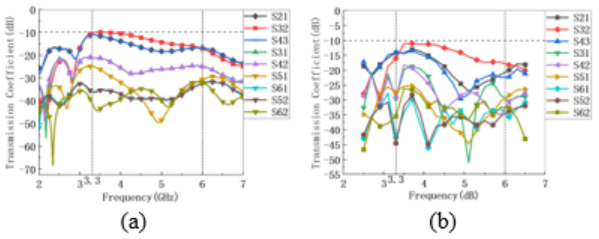

Fig. 11. Isolation levels between two antenna units. (a) Simulated. (b) Measured.

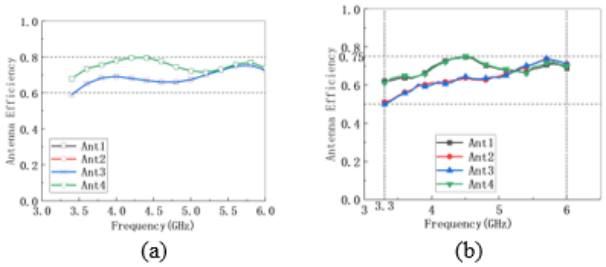

Fig. 12. Total antenna efficiencies of Ants1-4. (a) Simulated. (b) Measured.

phone antenna. The simulation results show that the total efficiency of the antenna is more than 60% in 3.3-6GHz band, and the maximum efficiency reaches 80%. The measured results show that the total efficiency of the antenna is more than 50% in 3.3-6GHz band, and the maximum efficiency is 75%. Figures 13 and 14 show the 2D pattern of antenna 1 and antenna 2 at three different frequency points in xoy plane respectively. The results are obtained by CST simulation. It can be seen from the figure that the antenna unit has a certain directivity according to the position of distribution, and the results of simulation and measurement also have good consistency. The result of comprehensive testing shows that the eight-element antenna system has good radiation receiving performance.

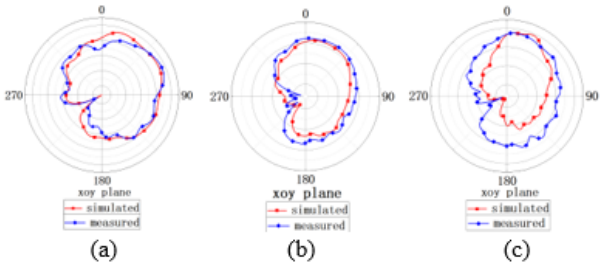

Fig. 13. Simulated and measured radiation patterns across the *xy* plane for Ant1. (a) at 3.6 GHz, (b) at 4.8 GHz, (c) at 5.6 GHz.

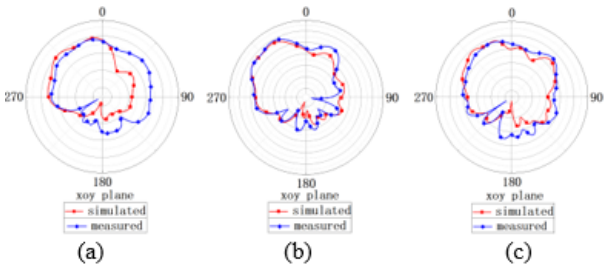

Fig. 14. Simulated and measured radiation patterns across the *xy* plane for Ant2, (a) at 3.6 GHz, (b) at 4.8 GHz, (c) at 5.6 GHz.

Figure 15 shows the Envelope Correlation Coefficient (ECC) simulation results of the antenna system [25–26]. Note that only necessary results are given in the figure. As can be seen from the figure, the ECC of the antenna system is all less than 0.08, indicating that each antenna unit of the antenna system has good channel independence. Table 2 compares the proposed eight-element MIMO array with some recently reported antenna designs. As can be seen, most designs cover only one or two narrow bands, and many broadband antennas are inefficient. In the antenna design proposed by us, on the premise that the isolation degree basically meets the requirements, not only the broadband design of the

antenna is realized, but also the overall efficiency and ECC of the antenna are ideal.

In order to realize the design of eight-element MIMO terminal antenna, reasonable spatial layout of the designed antenna pair is carried out, as shown in Fig. 16 (a). Since the two elements in the antenna pair are affected differently by the ground, the size of each element is fine-tuned to optimize the antenna pair. In addition, in order to reduce the coupling between antenna pairs on the same side, a zigzag-shaped decoupling gap is also designed between them. The size of the decoupling gap is given in Fig. 16 (a). Figure 16 (b) shows the comparison results of S32 antenna with or without the decoupling structure. As can be seen from the figure, after

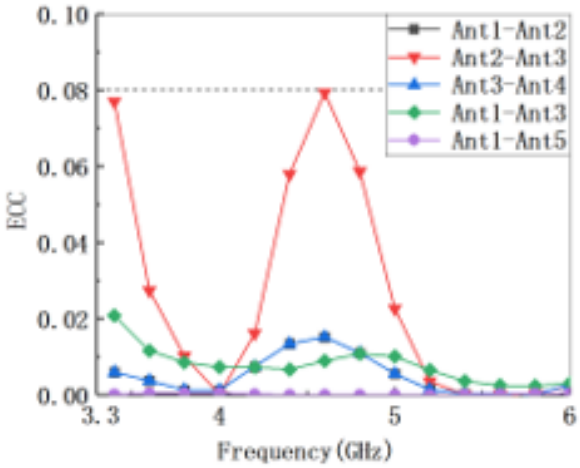

Fig. 15. The envelope correlation coefficient (ECC) of MIMO antenna.

Table 2: Performance comparison of the 5G MIMO terminal antennas

Design	AP	WB (GHz)	Isolation (dB)	Eff (%)	ECC
[5]	Y	3.4-3.6	>17	22-50	<0.1
[24]	Y	3.33-3.6	>14	52-65	<0.1
[9]	N	3.3-4.2 4.8-5	>12.5	LB 53-76 HB 62-79	<0.1
[10]	Y	3.3-3.6 4.8-5	>17.5	LB 49-68 HB 49-70	<0.1
[12]	Y	3.3-5	>12	31-88	<0.1
[21]	Y	3.3-7.5	>10	15-70	<0.0
Proposed	Y	3.3-6	>11	50-75	<0.8

Abbreviations: AP=Antenna Pair, WB=Working Band, Eff=Efficiency, LB=Low Band, HB=High Band.

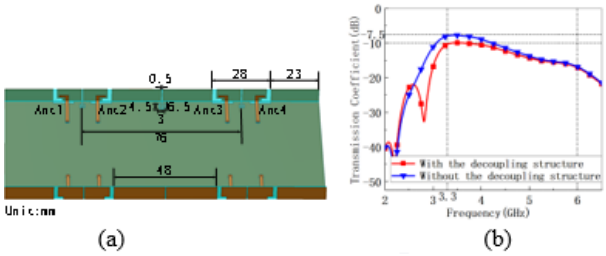

Fig. 16. Overall optimization design of antenna. (a) Spatial layout dimensions of antenna pairs. (b) Influence of decoupling structure on S32.

the decoupling structure is added, the isolation degree between antenna 2 and antenna 3 is improved to more than 10 dB.

IV. CONCLUSION

This paper presents an eight-element MIMO array for 5G terminals. The working bandwidth of the antenna ranges from 3.3 to 5.95 GHz (57.3%), fully covering n77/n78/n79 and WLAN 5 GHz band. According to the real antenna made and tested, the measured results are in good agreement with the simulation results. The isolation performance of the system is better than 11 dB, the total efficiency is higher than 50%, and the ECC is lower than 0.08. It has good MIMO performance and meets the performance requirements of modern mobile terminal antennas. It is a good MIMO antenna solution for 5G mobile terminals.

REFERENCES

[1] 3GPP specification series: 38series, 3GPP TS 38.101-1 v15.0.0, 2017. Available online at: http://www.3gpp.org/DynaReport/38-series.htm

[2] M. Ikram, N. Nguyen-Trong, and A. Abbosh, "Hybrid antenna using open-ended slot for integrated 4G/5G mobile application," *IEEE Antennas and Wireless Propagation Letters*, vol. 19, no. 4, pp. 710-714, Apr. 2020.

[3] L. Sun, H. Feng, Y. Li, and Z. Zhang, "Compact 5G MIMO mobile phone antennas with tightly arranged orthogonal-mode pairs," *IEEE Trans. Antennas Propag*, vol. 66, no. 11, pp. 6364-6369, Nov. 2018.

[4] Y. Li, C. Sim, Y. Luo, and G. Yang, "High-isolation 3.5 GHz eight-antenna MIMO array using balanced open-slot antenna element for 5G smartphones," *IEEE Trans. Antennas Propag.*, vol. 67, no. 6, pp. 3820-3830, Jun. 2019.

[5] Z. Ren, A. Zhao, and S. Wu, "MIMO antenna with compact decoupled antenna pairs for 5G mobile terminals," *IEEE Antennas and Wireless Propagation Letters*, vol. 18, no. 7, pp. 1367-1371, Jul. 2019.

[6] H. Piao, Y. Jin, and L. Qu, "A compact and straightforward self-decoupled MIMO antenna system for 5G applications," *IEEE Access*, vol. 8, pp. 129236-129245, Jul. 2020.

[7] A. Ren, Y. Liu, H. Yu, Y. Jia, C. Sim, and Y. Xu, "A high-isolation building block using stable current nulls for 5G smartphone applications," *IEEE Access*, vol. 7, pp. 170419-170429, Nov. 2019.

[8] D. Serghiou, M. Khalily, V. Singh, A. Araghi, and R. Tafazolli, "Sub-6 GHz dual-band 8 × 8 MIMO antenna for 5G smartphones," *IEEE Antennas Wireless Propag. Lett*., vol. 19, no. 9, pp. 1546-1550, Sep. 2020.

[9] L. Cui, J. Guo, Y. Liu, and C. Sim, "An 8-element dual-band MIMO antenna with decoupling stub for 5G smartphone applications," *IEEE Antennas Wireless Propag. Lett*., vol. 18, no. 10, pp. 2095-2099, Aug. 2019.

[10] Z. Ren and A. Zhao, "Dual-band MIMO antenna with compact selfdecoupled antenna pairs for 5G mobile applications," *IEEE Access*, vol. 7, no. 10, pp. 82288-82296, Oct. 2019.

[11] W. Hu, L. Qian, S. Gao, L.-H. Wen, Q. Luo, H. Xu, X. Liu, Y. Liu, and W. Wang, "Dual-band eight-element MIMO array using multi-slot decoupling technique for 5G terminals," *IEEE Access*, vol. 7, pp. 153910-153920, Oct. 2019.

[12] L. Sun, Y. Li, Z. Zhang, and Z. Feng, "Wideband 5G MIMO antenna with integrated orthogonal-mode dual-antenna pairs for metal-rimmed smartphones," *IEEE Trans. Antennas Propag*, vol. 68, no. 4, pp. 2494-2503, Apr. 2020.

[13] C. Sim, H. Liu, and C. Huang, "Wideband MIMO antenna array design for future mobile devices operating in the 5G NR frequency bands n77/n78/n79 and LTE band 46," *IEEE Antennas Wireless Propag. Lett*., vol. 19, no. 1, pp. 74-78, Jan. 2020.

[14] L. Sun, Y. Li, and Z. Zhang, "Wideband decoupling of integrated slot antenna pairs for 5G smartphones," *IEEE Trans. Antennas Propag*, vol. 69 no. 4, pp. 2386-2391, Apr. 2021.

[15] J. Guo, L. Cui, C. Li, and B. Sun, "Side-edge frame printed eight-port dual-band antenna array for 5G smartphone applications," *IEEE Trans. Antennas Propag*., vol. 66, no. 12, pp. 7412-7417, Dec. 2018.

[16] W. Jiang, B. Liu, Y. Cui, and W. Hu, "High-isolation eight-element MIMO array for 5G smartphone applications," *IEEE Access*, vol. 7, pp. 34104-34112, Mar. 2019.

[17] H. Chen, Y. Tsai, C. Sim, and C. Kuo, "Broadband eight-antenna array design for sub-6 GHz 5G NR bands metal-frame smartphone applications," *IEEE Antennas and Wireless Propagation Letters*, vol. 19, no. 7, pp. 1078-1082, Jul. 2020.

[18] H. Xu, H. Zhou, S. Gao, H. Wang, and Y. Cheng, "Multimode decoupling technique with independent tuning characteristic for mobile terminals," *IEEE Trans. Antennas Propag*., vol. 65, no. 12, pp. 6739-6751, Dec. 2017.

[19] A. Zhao and Z. Ren, "Multiple-input and multiple-output antenna system with self-isolated antenna element for fifth-generation mobile terminals," *Microw. Opt. Technol. Lett*., vol. 61, no. 1, pp. 20-27, Jan. 2019.

[20] A. Zhao and Z. Ren, "Size reduction of self-isolated antenna MIMO antenna system for 5G mobile phone applications," *IEEE Antennas Wireless Propag. Lett.*, vol. 18, no. 1, pp. 152-156, Jan. 2019.

[21] X.-T. Yuan, Z. Chen, T. Gu, and T. Yuan, "A wideband PIFA-pair-based MIMO antenna for 5G smartphones," *IEEE Antennas and Wireless Propagation Letters*, vol. 20, no. 3, pp. 371-375, Mar. 2021.

[22] L. Chang, Y. Yu, K. Wei, and H. Wang, "Orthogonally polarized dual antenna pair with high isolation and balanced high performance for 5G MIMO smartphone," *IEEE Transactions on Antennas and Propagation*, vol. 68, no. 5, pp. 3487-3495, May 2020.

[23] C. Deng, D. Liu, and X. Lv, "Tightly arranged four-element MIMO antennas for 5G mobile terminals," *IEEE Trans. Antennas Propag*., vol. 67, no. 10, pp. 6353-6361, Oct. 2019.

[24] Z. Xu and C. Deng, "High-isolated MIMO antenna design based on pattern diversity for 5G mobile terminals," *IEEE Antennas Wireless Propag. Lett*., vol. 19, no. 3, pp. 467-471, Mar. 2020.

[25] Y. Q. Hei, J. G. He, and W. T. Li, "Wideband decoupled 8-element MIMO antenna for 5G mobile terminal applications," *IEEE Antennas and Wireless Propagation Letters*, vol. 20, no. 8, pp. 1448-1452, Aug. 2021.

[26] X.-T. Yuan, W. He, K.-D. Hong, C.-Z. Han, Z. Chen, and T. Yuan, "Ultra-wideband MIMO antenna system with high element-isolation for 5G smartphone application," *IEEE Access*, vol. 8, pp. 56281-56289, Mar. 2020.

[27] M. O. Khalifa, A. M. Yacoub, and D. N. Aloi, "Compact 2x2 and 4x4 MIMO antenna systems for 5G automotive applications," *Applied Computational Electromagnetics Society (ACES) Journal*, vol. 36, no. 6, pp. 1943-5711, Nov. 2021.

[28] J. Su, Z. Dai, and J. Du, "A compact dual-band MIMO antenna for 5G mobile communications,"

Applied Computational Electromagnetics Society (ACES) Journal, vol. 34, no. 11, pp. 1943-5711, Nov. 2019.

Jiagang He was born in Xiangtan, Hunan province, China, in 1997. He received his Bachelor's degree from the College of Electronic Science and Technology, Hunan University of Technology, Zhuzhou, China, in 2019. He is now studying for a postgraduate degree at the College of Electronic Science and Technology, Hunan University. His research interests are terminal antenna and EMC.

Shichao Zhu received his Bachelor's degree from the School of Electrical and Automation Engineering, East China Jiaotong University, Nanchang, China, in 2020. He is currently pursuing a Master's degree at the College of Electrical and Information Engineering, Hunan University, Changsha, China, under the supervision of Prof. G. S. Li. His research interests include reconfigurable antennas, electromagnetic metamaterials and their antenna applications.

Jie Yu was born in Xinyang, Henan province, China, in 1998. He received his Bachelor's degree in Optoelectronic Information Science and Engineering from Changsha University of Science and Technology, Changsha, China, in 2019. He is currently working as a postgraduate at Hunan University. His research interest is liquid antennas.

Hao Li is an associate professor at the College of Electrical and Information Engineering, Hunan University, Changsha, China. His research interests include microwave dielectric materials and devices for microwave communication.

Gaosheng Li (M'08, SM'19) received his B.S. degree in Electromagnetic Fields and Microwaves in 2002 from the National University of Defense Technology (NUDT), Changsha, China. His M.S. and Ph. D. degrees were in Electronic Science and Technology from the same university, in 2004 and 2013, respectively.

He was with NUDT as a Teaching Assistant from 2004 to 2006, as a Lecturer from 2006 to 2011, and then as an Associate Professor from 2011 to 2017. He joined Hunan University as a Professor in 2018. From 2014 to 2016, he was with Nanjing University of Aeronautics and Astronautics (NUAA) and Wuxi Huace Electronic Systems Co., Ltd., China as a postdoctoral Research Fellow. From 2016 to 2017, he was a Visiting Scholar at the University of Liverpool (UoL), United Kingdom, sponsored by the China Scholarship Council (CSC). He is a Senior Member of the IEEE. His research interests include antennas and propagation (AP), electromagnetic compatibility (EMC), and wireless propagation and microwave systems.